Behavior of structures equipped with variable friction dissipative systems

Liborio Cavaleri
Department of Engineering, University of Palermo, Palermo, 90128, Italy, liborio.cavaleri@unipa.it

Mario Di Paola
Department of Engineering, University of Palermo, Palermo, 90128, Italy, mario.dipaola@unipa.it

Marco Filippo Ferrotto
Department of Engineering, University of Palermo, Palermo, 90128, Italy, marcofilippo.ferrotto@unipa.it

Vincenzo Sucato
Department of Engineering, University of Palermo, Palermo, 90128, Italy, vincenzo.sucato03@unipa.it

Abstract: Usually, in order to mitigate the stresses in framed structures, different strategies are used. Among them, the base isolation, the viscous dampers and tuned mass dumpers have been widely investigated.
In this paper a strategy of energy dissipation by friction is proposed, that is a braking system borrowed from the mechanical engineering. The constitutive law of such system is linearly dependent on the displacement of the device - therefore on the interstorey displacement of structures - and depends also on the signum function of the interstorey velocity.
The feasibility of the braking system, the amount of energy that can be dissipated and the overall performances of structures equipped with these type of systems are studied in detail in view of provide adequate levels of energy dissipation, being effective and not dangerous for structures that request limited interstorey drifts.

Keywords: Dissipative systems; variable friction dissipative device; Structural dynamics

1. Introduction

Structural vibration control involves the use of dissipation devices to reduce excessive vibration during winds or earthquakes to limit damage in the structural members. These devices can be used in the case of new constructions as well as for the retrofitting of existing buildings exploiting the effect of adding energy dissipation capacity.

The purpose of using these kind of strategies is that the structure must remain in the elastic range so that the bearing frames can be designed considering reduced seismic actions, while the task of facing the majority of the seismic loads is demanded to bearing isolators or to dissipative systems.

Bearing isolators are interposed between the foundation and the superstructure for the decoupling of the frequencies coming from the ground motion and the superstructure to achieve a longer period of vibration that makes the seismic excitation to be much lower (Ferrotto et al. 2019, 2020). Typical bearing isolators

are elastomeric and sliding devices. Very often these two systems are used together to improve their efficiency (Braga and Laterza, 2004). Base isolation is mainly used for new buildings since for the case of existing structures this approach is very expensive and involves significant structural modifications.

Dissipative systems are used to provide to the structures supplementary energy dissipation by means of devices that can be of different types. Among the most known there are fluid viscous dampers, yielding dissipaters, hysteretic, viscoelastic and friction dampers. In the case of existing buildings, the installation of these devices may not require excessive modifications.

Hysteretic yielding dampers are generally made of steel. They can be designed to reach the yielding strength in bending, shear or axially (Teruna et al., 2015). The yielding of the hysteretic dampers is designed to be reached before the yielding of the structural members. These systems provide also an increasing of stiffness and strength to the structure.

Visco-elastic dampers are generally formed by two layers of polymer bonded between a central driving plate and two outer plates. The damping force is linearly velocity dependent and produce an elliptical force-displacement function where the inclination of the major axis corresponds to the stiffness of the device.

Fluid viscous dampers are very efficient because of their velocity-dependent behavior. Dampers force are out of phase with the relative displacement and therefore the structural restoring forces; for this reason, the peak forces of a viscous damper does not add to the peak restoring forces; they can be designed with characteristics that do not change the stiffness of the structure (Alotta et al., 2016).

Friction dampers are special dissipative devices that act as fuses, having force-displacement behavior independent by the velocity and the frequency. The task of these devices is to limit the force on the members. Each damper has a typical Coulomb-friction law and it is manufactured to slip at a specified force, within a specified tolerance over the specified travel. The slip force is controlled by the tension in bolts holding together the sliding elements (Bhaskararao and Jangid, 2006).

In addition to the traditional supplementary dissipative systems, in the last period, a number of innovative energy dissipating devices have been studied (Cancellara et al., 2019). Dal Lago et al. (2018) presented a study of precast concrete structures with energy dissipating cladding panel connection systems with friction-based or plasticity-based devices interposed in between adjacent cladding panels or between the panels. Cook et al. (2018) proposed a dissipative system (named by the authors as Grip ‘n’ Grab GnG device) composed by a tension-only device with a ratcheting function to improve the behavior with respect to the buckling restrained braces (BRBs). In fact, the system proposed by the authors eliminates residual compressive forces and removes the need for buckling restraint. The device is designed to be used in conjunction with a dissipater, and energy dissipation in the GnG-dissipater system can be provided by various mechanisms such as yielding or friction. Bagheri et al. (2019) studied a cable bracing system comprising a pre-stressed cable and a drum interacting via frictional contact for lateral resistance of structures.

In this paper a braking system borrowed from the mechanical engineering is studied and designed as innovative method to be applied for the energy dissipation on moment resisting frame structures. The constitutive law of such system is linearly dependent on the displacement of the device and therefore on the interstorey displacement and depends on the signum function of the interstorey velocity.

The feasibility of the braking system, the amount of energy that can be dissipated and the overall performances of structures equipped with these type of systems are studied in details in view of provide adequate levels of energy dissipation, being effective and not dangerous for structures that request limited interstorey drifts.

2. Model for variable friction dissipative (VFD) device

The variable friction damper proposed in this study provides dissipative capacity as a function of two components: the first one, governed by pure friction, is constant and is a function of the signum of the velocity (typical Coulomb-friction law), while the second component depends on the relative displacement (in absolute value) and by the signum of the velocity. The latter is governed by a linear law that increases the dissipative force as the displacement increases and decreases as the displacement decreases until it reaches zero for relative zero displacements. In other words, the load-displacement response of the system is linear due to the existence of frictional contact as well as geometrical effects and it consists of two phases: a linear phase before gross slipping with a relatively specific force followed by a linear phase with gradually increasing stiffness (i.e. hardening). The mechanical model of the variable friction damper (VFD) device is shown in Fig. 1.

The device is composed by different components. In detail, two steel plates are fixed to the bottom of the beam at the upper floor, while an intermediate steel device is connected to the lower steel braces. The central device slides along the internal surfaces of the external plates that are bolted with a given prestressing induced by tightening (according to the classic friction damper devices).

The peculiarity of the novel device is that the internal surfaces of the two plates are inclined by a certain angle with respect to a horizontal sliding surface. This causes that the central device is forced to a convex funnel-shaped surface. This geometrical configuration generates additional restoring forces with the increasing of the relative outwards displacements of the central device. The tightening level of the bolts acts for the constant friction component, while the convex funnel-shaped surface provides an additional restoring force depending on the level of displacement.

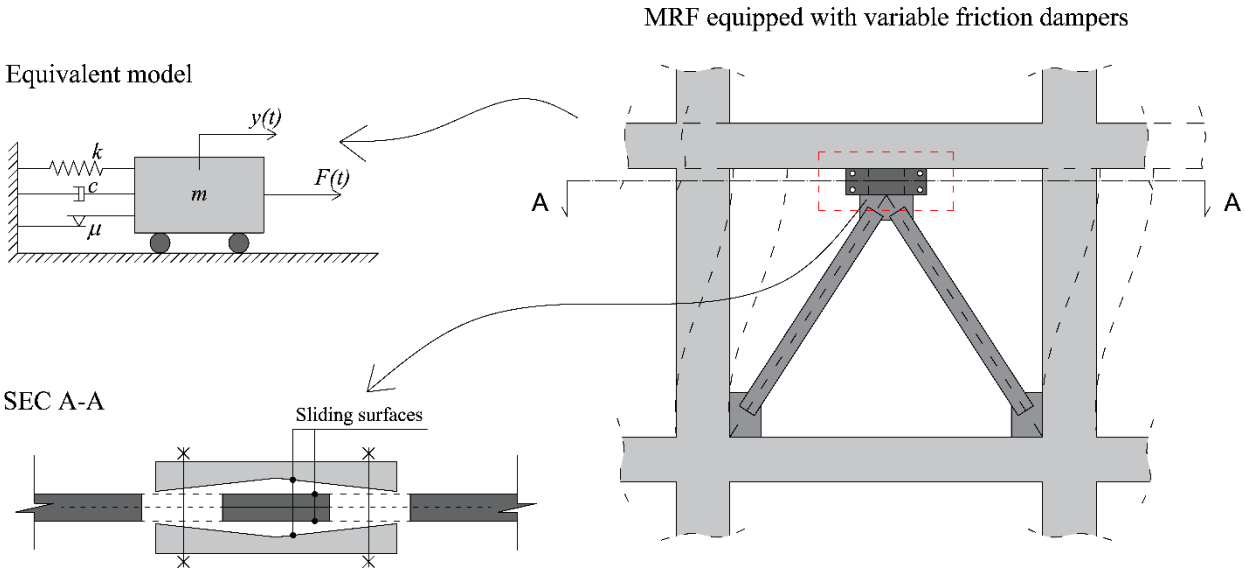

Figure 1. Mechanical model of VFD.

The governing equation of the variable friction damper (VFD) can be expressed as follow:

$$F = c_0 \cdot sign(\dot{x}) + c_1 \cdot |x| \cdot sign(\dot{x}) \tag{1}$$

where F is the dissipative force, $sign(\dot{x})$ is the signum function of the velocity, x is the relative displacement and c_0 and c_1 are constants. The first constant (c_0) depends by the pure friction like a constant brake system, while the second constant (c_1) depends on the shape and on the type of material used so it can act as a constant brake system but influenced by the relative displacement raised by the system during the increasing of the displacement.
In Eq. (1) the first dissipative component represents the constant friction damper (CFD) constitutive law. In Fig. 2 a comparison is shown in terms of load-displacement (Fig. 2a) and cycle-displacement (Fig. 2b) for CFD and VFD with and without the CFD component respectively. In detail, it can be seen that, while the force of the CFD is constant after the activation of the sliding, the force of the VFD is characterized also by initial normal stress at the interface equal to the slipping force (or zero if c_0=0), and the maximum dissipative force is attained at maximum displacement.

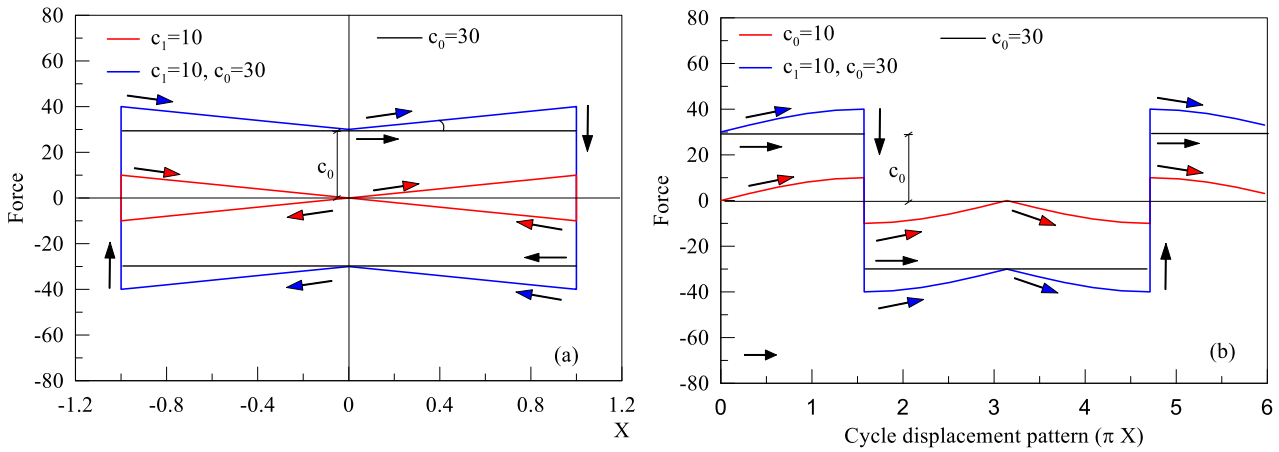

Figure 2. Comparison between VFD and FVD.

3. Implementing on a SDOF model

In this paper, a comparison is proposed on systems that can be modelled as single degree of freedom (SDOF) equipped alternatively with CFD and VFD. The seismic input is previously assigned. The responses are compared for a given level of additional maximum dissipation force to study the feasibility of applying the novel device.
The following equation of motion represents the behavior of the investigated systems:

$$\ddot{x} + 2\varsigma\omega\dot{x} + \frac{F_d}{m} + \omega^2 x = -\ddot{x}_g \tag{2}$$

where F_d is the dissipative force, m is mass, x is the displacement (the upper dot means time derivative), ς is the damping factor and ω^2 is the square own frequency obtained by dividing the stiffness by the mass. Moreover, $\ddot{X}_g$ is the external input in terms of ground accelerations and is modelled as a zero mean Gaussian white noise process characterized by the correlation function $R(\tau)$ given by:

$$R(\tau) = E\left[\ddot{X}_g(t)\,\ddot{X}_g(t+\tau)\right] = 2\pi S_0 \delta(\tau) \tag{3}$$

In Eq. (3) $E[\cdot]$ is the average operator, t means time, τ is a time delay, $\delta(\tau)$ is the Dirac's delta and S_0 is the Power Spectral Density of $\ddot{X}_g$.

4. Numerical application

To investigate on the mechanical and structural performances of the device, a series of time-history dynamic analyses are performed, starting from the response of the SDOF model with no dissipater in terms of displacements, velocities and the restoring forces. Then, the effect of using the VFD device in the reduction of the displacements was studied for different levels of additional dissipating forces designed as a ratio of the elastic restoring force. In detail the design procedure has been established as follows:

- Defining of the maximum dissipative force for the constant friction damper (CFD) (fixing c_0 in Eq. 1) as a ratio of the maximum elastic restoring force of the damped system;
- Performing the analysis to calculate the dynamic response (displacement, velocity, restoring force);
- Defining the linear variable part of the friction dissipater (VFD) (Eq. (1) fixing c_0 as for the CFD and c_1 to reach the 50% and the 100% of the pure friction maximum force respectively (Fig. 3);
- Performing the analysis to observe the differences in the dynamic response compared with the case of constant friction.

In addition to what above described, the efficiency of the VFD device has been investigated by keeping the same mechanical characteristics of the dissipater and varying the seismic input, using an accelerogram having higher peak ground acceleration (PGA). In doing so, an important consideration need to be pointed out that highlight the importance of the proposed novel device: differently from the constant friction damper (CFD) that provides always the same damping force regardless the intensity of the seismic input, the variable friction damper (VFD) take advantage in giving high dissipating force as much as the structure experience high displacements (that is the case of higher seismic inputs).

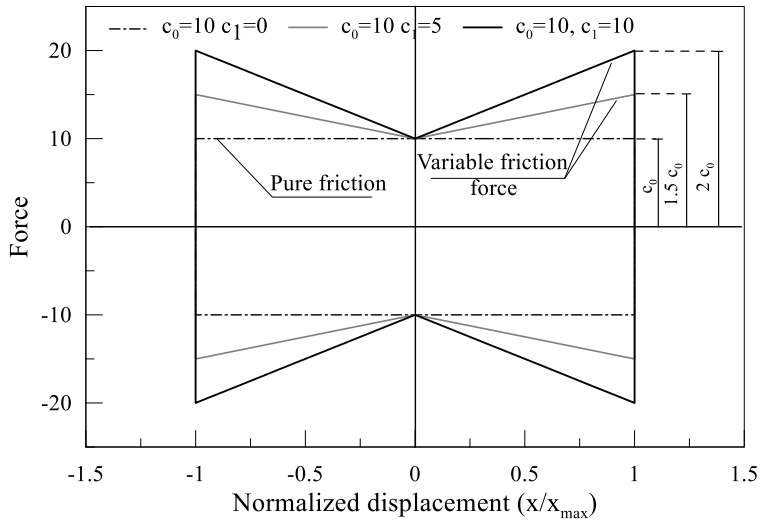

Figure 3. Case study for the VFD.

4.1. CHARACTERISTICS OF THE MODEL AND SEISMIC INPUT

The SDOF model was obtained starting from a single storey 3D reinforced concrete moment resisting frame structure of 4 meters' height, having columns with section dimension of 0.3 m x 0.5 m with the major inertia axis oriented along the direction of the seismic input. The modulus of elasticity of the reinforced concrete was assumed 30 GPa and a uniform distributed mass of 36 tons has been assigned to the floor. The system is shown in Fig. 4. For a given natural damping coefficient of 0.05, the dynamic characteristics of the SDOF model can be summarized as follows:

$$k = 0.5 \cdot 4\frac{12EI}{H^3} = 35156250\,\text{N/m}; \qquad \omega = \sqrt{\frac{k}{m}} = 31.25\,\text{sec}^{-1}; \qquad T = \frac{2\pi}{\omega} = 0.2\,\text{sec} \tag{4}$$

being k, ω and T the lateral stiffness, the own frequency and the vibration period respectively.

The seismic input was defined by two stationary accelerograms of 25 seconds (having the probabilistic characteristics expressed by Eq. 3), whose power spectral density S_0 have been fixed to obtain a peak ground acceleration (PGA) of 4.83 m/s^2 and 11.28 m/s^2 (corresponding to 0.5 g and 1.15g respectively). The dynamic response obtained from the first seismic input of 0.5g was used to design the dissipaters; then, the second seismic input of 1.15 g was used to investigate on the efficiency for seismic inputs higher than that used for the design. The accelerograms and the response spectrum curves are shown in Fig. 5a-b respectively.

Three set of analyses were performed beside the case of system without friction damper. In each set, the pure friction was maintained constant to exhibit a force approximately equal to 5%, 10% and 20% of the maximum restoring force of the system without friction damper respectively. The variable friction was varied to have the maximum variable component of the friction force about 15% of the maximum restoring

force of the system not with no damper. The analysis cases are summarized in Table 1 (the meaning of symbols and letters are explained in the next section).

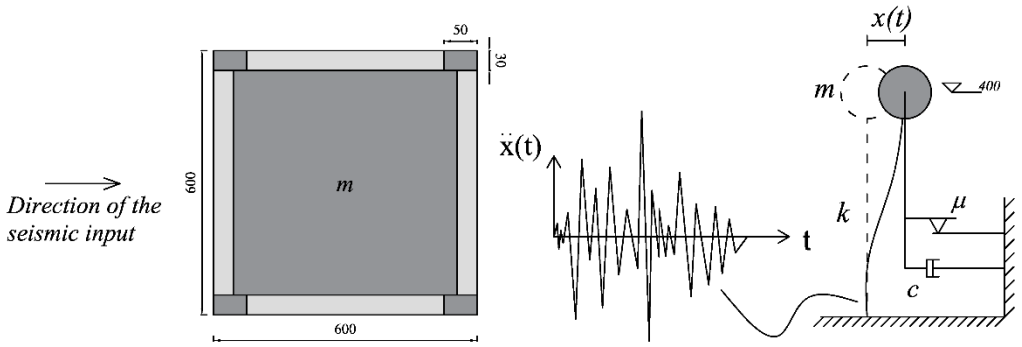

Figure 4. SDOF model.

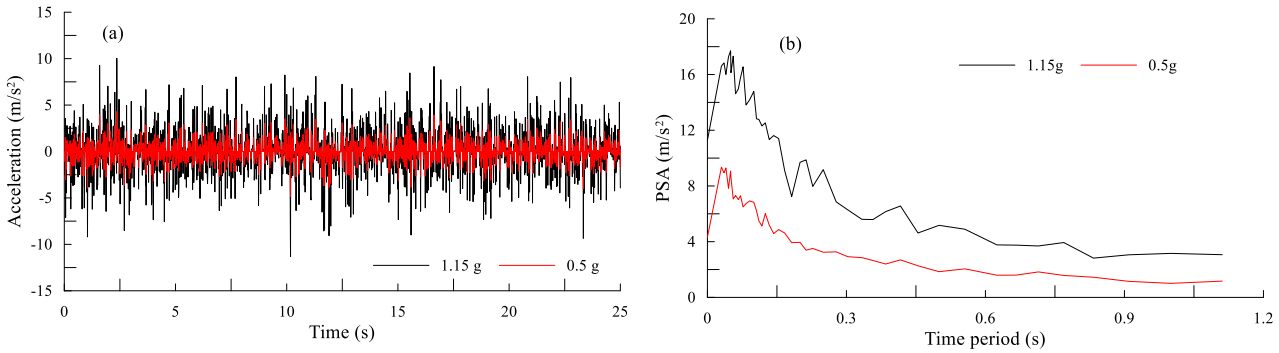

Figure 5. Accelerograms (a); Response spectra (b).

4.2. ANALYSIS RESULTS

Time-history analyses were performed calculating the dynamic responses. The analysis cases are labeled with the letter A and B for the accelerograms with PGA of 0.5g and 1.15g respectively. The results for the case A are summarized in Table 1 where number that follows A refers to ratio (in percentage) between the pure friction force and the maximum restoring force while the roman numbers I and II correspond respectively to a maximum variable friction force half and equal to the pure friction. For example, A-5 refers to a system exhibiting a constant friction force equal to 5% of the maximum restoring force exhibited by the system without dissipater (A) and without the contribution of the variable friction component of the force (c_1 = 0), A-5-I refers to a system exhibiting a constant friction of 5% and maximum variable component of friction equal to 50% of the constant friction, A-10-II refers to a system exhibiting a constant

friction of 10% and maximum variable component of friction equal to 100% of the constant friction and so on. The restoring and the damping forces are normalized with respect to the mass of the system.

Table I. Analysis scheme and results for the SDOF model equipped with VFD.

	Restoring force RF		Friction coefficients		Friction force FF		Dissipated energy	
CASE ANALYSIS	Maximum normalized (m/s^2)	Ratio "without VFD/ withVFD"	c_0 (m/s^2)	c_1 ($1/s^2$)	Maximum normalized (m/s^2)	FF/RF (%)	E	%
A	4.230	1.000	0	0	0	0	0.272	1.000
A-5	2.830	0.669	0.145	0	0.145	0.05	0.341	1.253
A-5-I	2.470	0.584	0.145	50	0.266	0.11	0.373	1.371
A-5-II	2.180	0.515	0.145	100	0.361	0.17	0.401	1.475
A-10	2.194	0.519	0.225	0	0.225	0.10	0.362	1.332
A-10-I	2.070	0.489	0.225	50	0.324	0.16	0.385	1.417
A-10-II	1.899	0.449	0.225	100	0.42	0.22	0.408	1.499
A-20	1.850	0.437	0.370	0	0.37	0.20	0.405	1.490
A-20-I	1.740	0.411	0.370	50	0.463	0.27	0.418	1.536
A-20-II	1.720	0.407	0.370	100	0.552	0.32	0.439	1.613

Figure 6 and Fig. 7 show the results in terms of displacements, velocities and restoring forces for the cases A-5, A-5-I, A-5-II and A-20, A-20-I, A-20- II on a 25 sec time window. The effectiveness of the dissipation device is evident and shows a considerable reduction in the dynamic response. Starting from the system with no VFD and analyzing the case with additional dissipation of 5%, a maximum displacement of 0.0043 m, decreasing to 0.0029 m, 0.0025 m and 0.0022 m for A-5, A-5-I, A-5- II is observed, showing a gradually marginal reduction. In the case of additional dissipation of 20%, a maximum displacements of 0.0021 m, 0.00185 m and 0.00181 m for cases A-20, A-20-I, A-20-II is obtained.

The relative reduction of the displacement (and therefore of the elastic restoring force) is higher in the case of additional dissipation of 5%, while the relative reduction is lesser for higher values of dissipation forces. These considerations give a preliminary idea about the efficiency of the target dissipation levels to be reached.

In Fig. 8, the comparisons between the restoring forces and the force experienced by the dissipaters are shown for a time interval between 10 and 11 seconds for the analysis cases A-5 and A-20 (for CFD and VFD). Moreover, Fig. 9 shows for a wide time interval (from 10 to 13 seconds) the dynamic response for the analysis cases A-10 and A-10-II to highlight the variation of the dynamic response depending on the type of friction device used (constant or linear variable).

Based on the results obtained by the time-history analyses, some considerations can be drawn. With a low level of constant additional friction dissipative force (as for the case A-5 in which the friction force is 5% of the elastic restoring force) given to the constant part, by using the novel device, higher dissipative forces can be obtained. In detail, the range varies from 5% to 10% to 17% depending on weather a device with capacity of 50% or 100% of the constant friction is used. If the case A-10 is analyzed, the novel device provides, starting from the 10%, 16% and 22% for the cases A-10-I and A-10-II respectively. Finally, for the case of 20% of dissipative forces, the 27% and the 32% are obtained for the cases A-20-I and A-20-II

respectively. However, as for the displacements, the increasing of the ratio between the force experienced by the friction dissipater and the elastic restoring force is marginal showing a non-linear trend. This confirms what assessed about a definition of an optimal threshold value to be defined for the additional dissipation. The results of what above described are shown in Tab. 1 and Fig. 10a. Fig. 10b shows the normal probability distribution of the displacements obtained by the analyzes. It can be noted that the dispersion in the case of system with no additional dissipation is much higher than in the case with VFD. The dispersion reduces with the increasing of the dissipation, giving information on the reduction of the range of displacements.

In Fig. 11, a comparison is made in terms of force-displacement cycles obtained in the case of CFD (Fig. 11a), in the case of VFD (Fig. 11b) with a capacity of 0.42. The case analyses are A-10 and A10-II respectively.

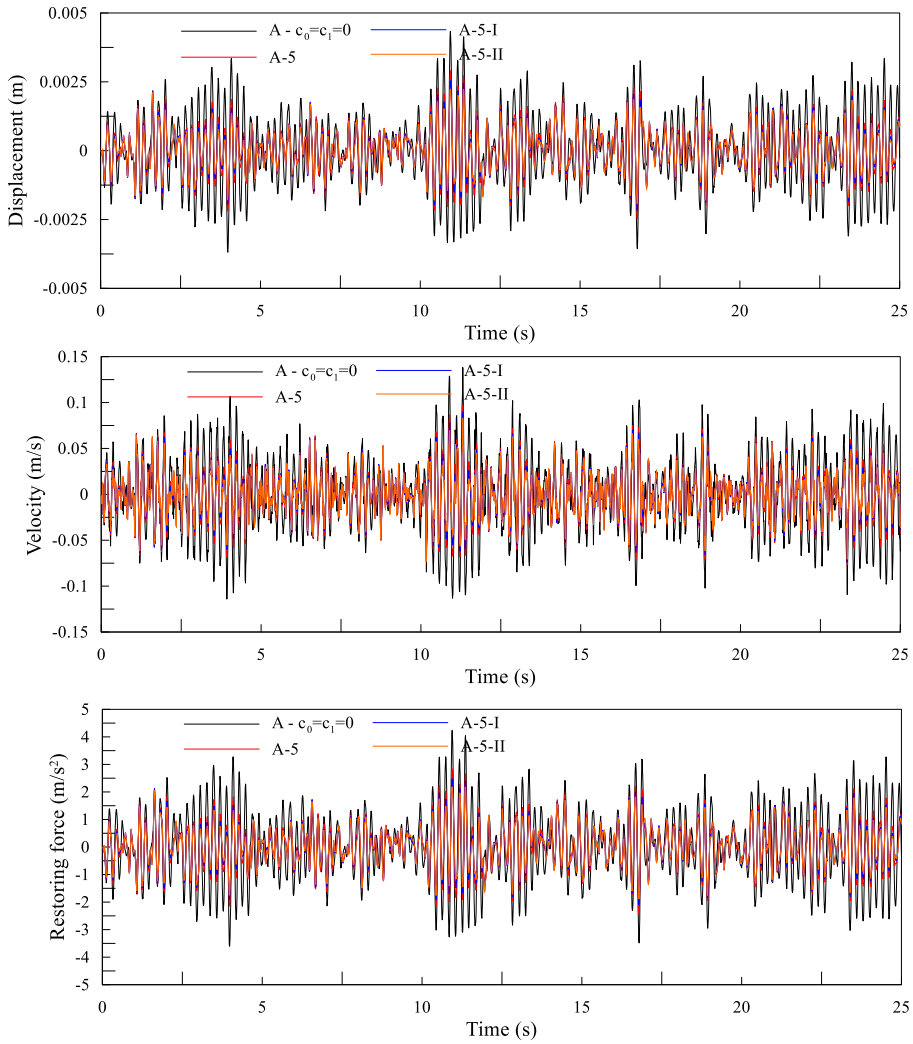

Figure 6. Time-history results for the case of constant friction dissipater (CFD) and variable friction dissipater (VFD) for the case analysis A, A-5, A-5-I and A-5-II.

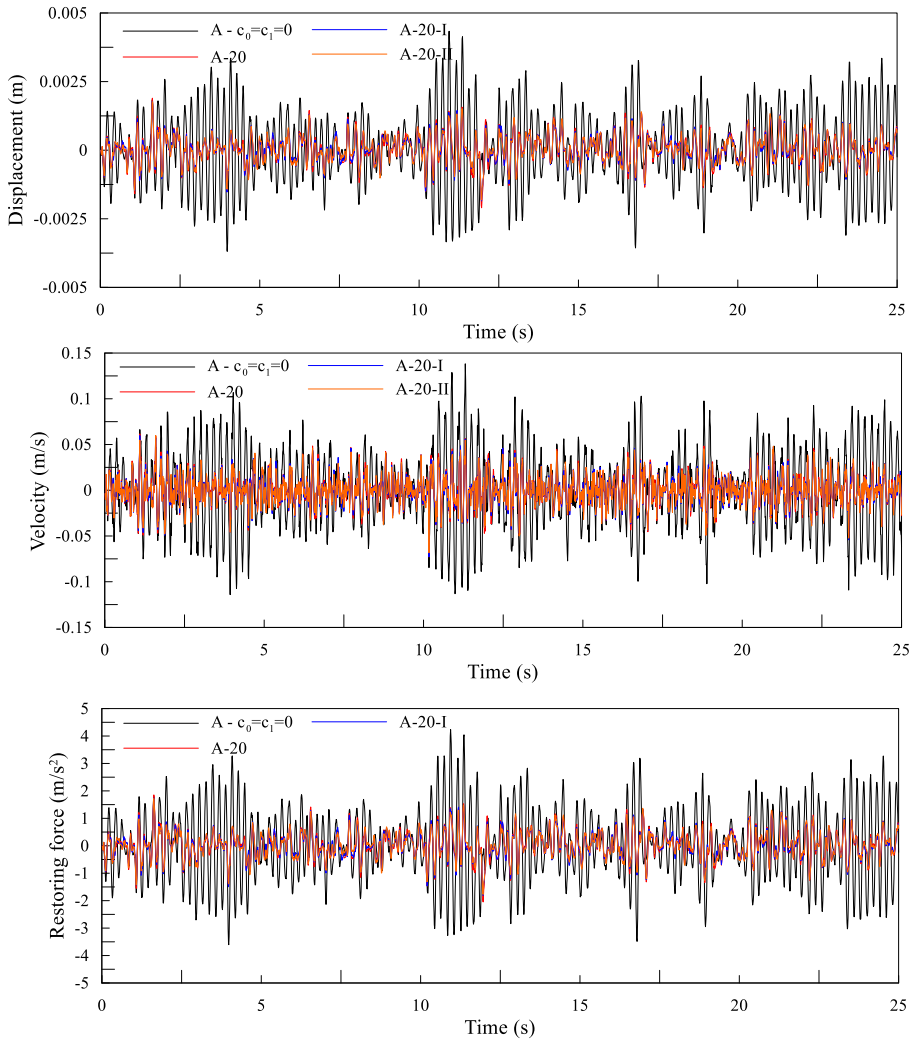

Figure 7. Time-history results for the case of constant friction dissipater (CFD) and variable friction dissipater (VFD) for the case analysis A, A-20, A-20-I and A-20-II.

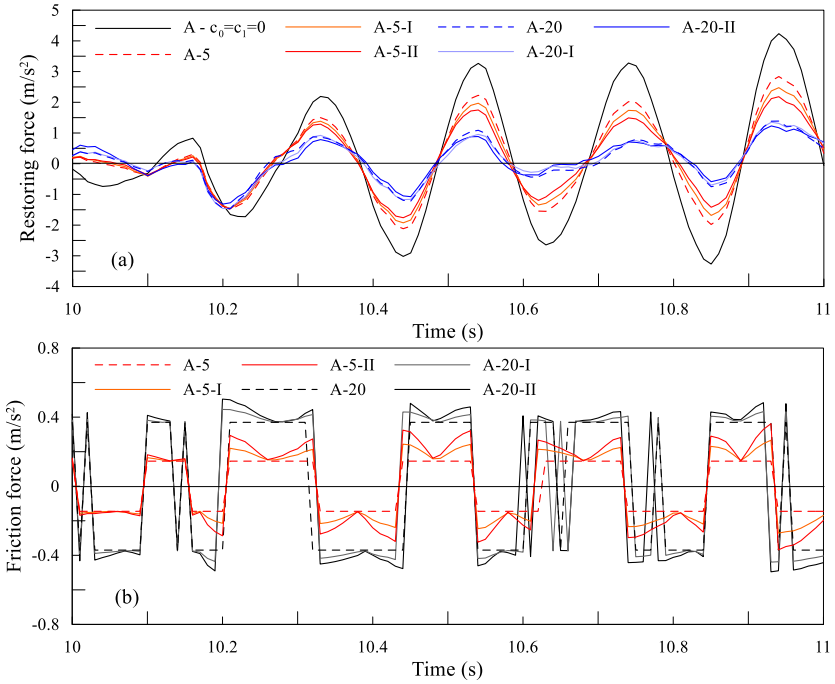

Figure 8. Restoring force and friction forces for time interval of 10-11 seconds for the various analysis cases.

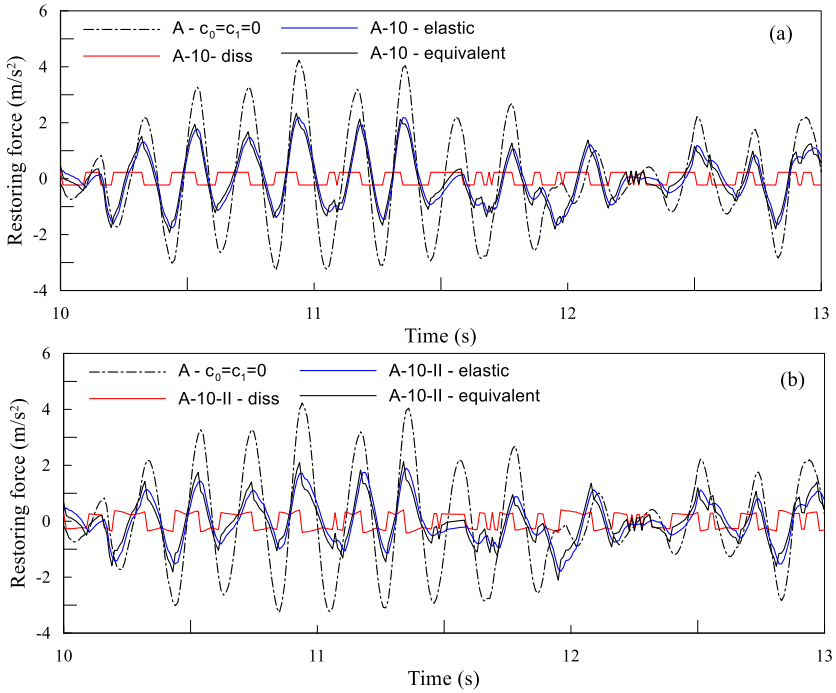

Figure 9. Response of the system equipped with CFD (a) and VFD (b).

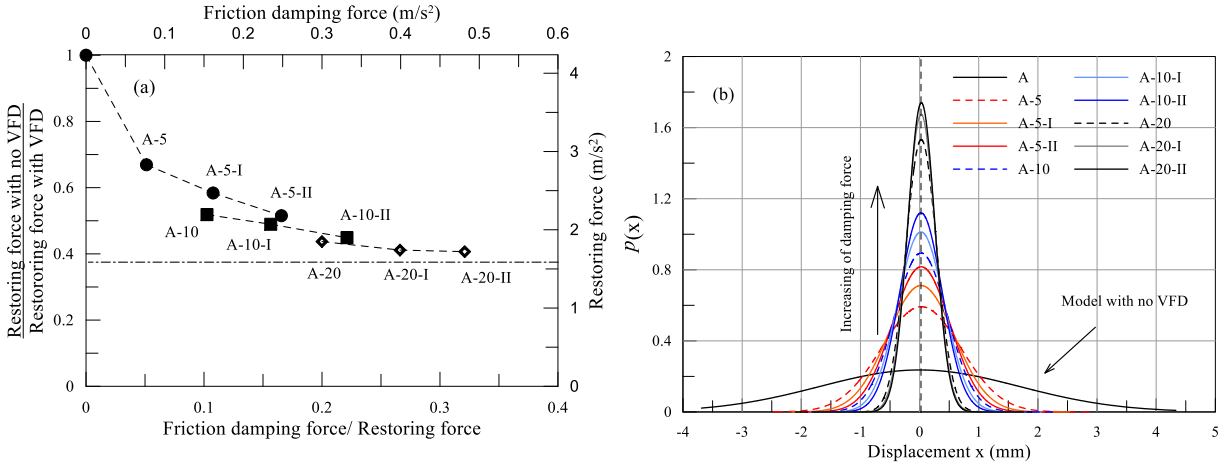

Figure 10. Reduction of the restoring force with the increasing of the damping force (a); Normal distribution of the displacements for the various analyses cases (b).

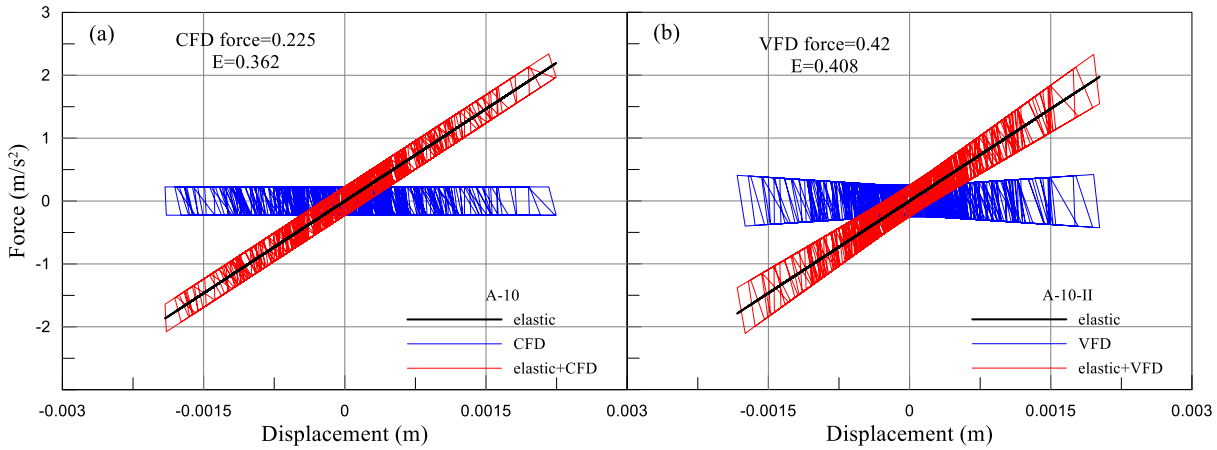

Figure 11. Force-displacement cycles: CFD (a); VFD (b).

An important consideration that can be drawn is that by using the novel device it is not necessary to define high friction forces to reach high levels of dissipation but it is possible to design a device that exploits the geometrical effect to increase the dissipative force with the increasing of the displacements. This effect is clearly highlighted in Fig. 12 a, where the maximum forces of the dissipaters are shown for the two seismic input A and B respectively with PGA of 0.5g and 1.15g. It is clearly shown that when the seismic input increases and, consequently, the displacements are higher, the maximum force of the VFD are higher, confirming the high efficiency of the VFD devices compared with the CFD ones. In other word, the constant friction damper (CFD) provides always the same damping force regardless the intensity of the seismic input, while, by using variable friction dampers (VFD) the advantage is obtained in giving to the

structure high dissipating force as much as the structure experience high displacements. Therefore, the higher is the displacement that the system tends to reach, the higher is the force exhibited by the dissipater. Obviously, the relative travel of the dissipater after the slipping force has to be accurately defined during the design.

The same considerations about the displacement reductions (Fig. 12b) can be obtained also in the case of the seismic input B (1.15g). The maximum displacement drops from 0.01 m for the system with no dampers to 0.006 m and 0.005 m for the case analysis B5-II and B20-II respectively, indicating a marginal reduction of the displacement for higher values of damping forces.

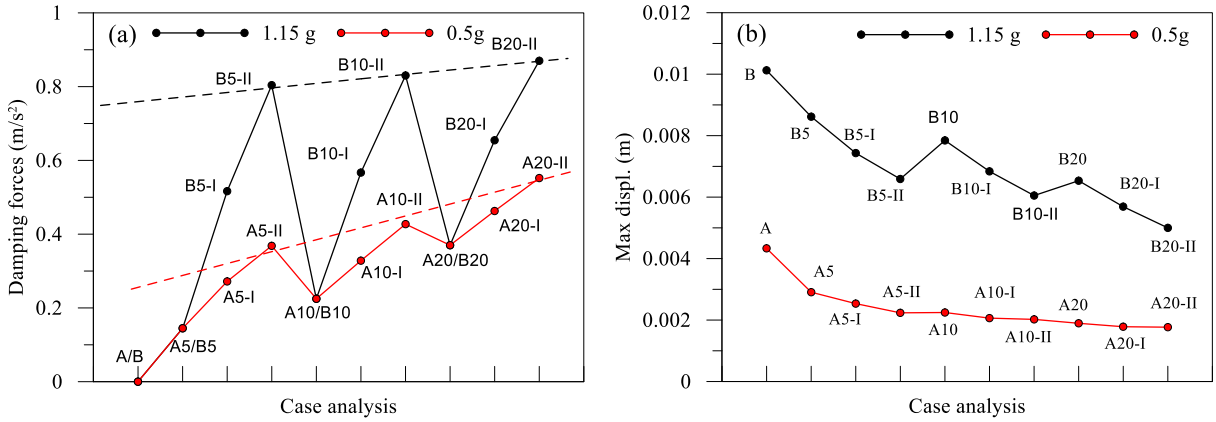

Figure 12. Maximum (a) friction forces and (b) displacements for seismic input A (0.5g) and B (1.15g)

5. Conclusions

In this paper a braking system borrowed from the mechanical engineering was presented as innovative method to be applied for the energy dissipation on moment resisting frame structures. The constitutive law of such a system is linearly dependent on the displacement of the device and therefore on the interstorey displacement and depends on the signum function of the interstorey velocity.

The feasibility of the braking system, the amount of energy that can be dissipated and the overall performance of structures equipped by these type of systems was studied in details for different intensities of the seismic input. The novel device resulted to be very efficient in terms of the reduction of the dynamic response, showing a capability of providing higher amount of dissipated energy and a significant reduction of the interstorey displacements. The system is certainly worthy of attention as it allows to reach greater dissipation forces than the classic friction dissipaters, exploiting the geometric effects of the device which causes the modification of the constitutive law by assigning a linear component dependent on the relative displacement.

References

Alotta, G., Cavaleri, L., Di Paola, M., Ferrotto, M.F. Solution for the Design and Increasing of Efficiency of Viscous Dampers. *The Open Construction and Building Technology Journal*, 10, (Suppl 1: M6):106-121, 2016.

Bagheri, S., Shishvan, S.S., Barghian, M. and Baniahmad, B. A new energy dissipative cable bracing system. *Advances in Structural Engineering*, 22(14):3134–3146, 2019.

Bhaskararao, A.V., Jangid, R.S. Seismic analysis of structures connected with friction dampers. *Engineering Structures*, 28 (2006) 690–703

Braga, F., Laterza, M. Field testing of low-rise base isolated building. *Engineering Structures* 26:1599-1610, 2004.

Cancellara, D., De Cicco, S., De Angelis, F. Assessment and vulnerability reduction of under-designed existing structures: Traditional vs innovative strategy. *Computers and Structures* 221:44–64, 2019.

Cavaleri, L., Di Trapani, F., Ferrotto, M.F. Experimental determination of viscous dampers parameters in low velocity ranges. *Ingegneria Sismica*, 34(2):64-74, 2017.

Cook, J., Rodgers, G.W. and MacRae, G.A. Design and Testing of Ratcheting, Tension-Only Devices for Seismic Energy Dissipation Systems. *Journal of Earthquake Engineering*, 2018. DOI: 10.1080/13632469.2018.1441765.

Dal Lago, B., Biondini, F., Toniolo, G. Seismic performance of precast concrete structures with energy dissipating cladding panel connection systems. *Structural Concrete*, 19: 1908–1926, 2018. https://doi.org/10.1002/suco.201700233.

Ferrotto, M.F., Asteris, P.G., Cavaleri, L. Strategies of Identification of a Base-Isolated Hospital Building by Coupled Quasi-Static and Snap-Back Tests, *Journal of Earthquake Engineering*, 2020, DOI: 10.1080/13632469.2020.1824877;

Ferrotto, M.F., Cavaleri, L., Di Trapani, F., & Castaldo, P. Full scale tests of the base-isolation system for an emergency hospital. In COMPDYN 2019 7th International Conference on Computational Methods in Structural Dynamics and Earthquake Engineering 2019 - vol.1 (pp. 2012-2025). M. Papadrakakis, M. Fragiadakis (eds.). Crete, Greece, 24–26 June 2019.

Teruna, D.R., Majid, T.A. Budiono, B. Experimental Study of Hysteretic Steel Damper for Energy Dissipation Capacity. *Advances in Civil Engineering*, 631726, 12 pages. 2015. http://dx.doi.org/10.1155/2015/631726.